Available online at www.sciencedirect.com
SCIENCE DIRECT®
Radiation Measurements 41 (2006) 253–256
Radiation Measurements
www.elsevier.com/locate/radmeas

Comparison among different models of track growth and experimental data

D. Nikezic[a,*], D. Kostic[a], C.W.Y. Yip[b], K.N. Yu[b]

[a] *Faculty of Science, University of Kragujevac, R. Domanovic 12, 34000 Kragujevac, Serbia and Montenegro*
[b] *Department of Physics and Materials Science, City University of Hong Kong, Tat Chee Avenue, Kowloon, Hong Kong*

Received 2 February 2005; received in revised form 15 August 2005; accepted 6 September 2005

Abstract

The lengths of major axes of the alpha-particle track openings in CR-39 detectors were calculated by using four different models of track growth. Special computer programs were prepared for each of the models under comparison. Some differences were found among the results from the various models considering the wide ranges of incident angles, energies and removed layers during chemical etching. Systematical comparisons with experimental data for various incident angles and energies up to 5 MeV were also performed.

Keywords: Alpha particle; CR-39 detector; Track growth

1. Introduction

Development of tracks in materials during etching has attracted much attention for a long time (e.g., Henke and Benton, 1971; Paretzke et al., 1973; Somogyi and Szalay, 1973; Somogyi, 1980; Fromm et al., 1988; Fews and Henshaw, 1982; Ditlov, 1995; Nikezic and Kostic, 1997; Nikezic and Yu, 2003a, 2004). Formation of a track as a result of the incidence of an ion is due to the simultaneous acting of the etching solution with two etching rates, i.e., the variable rate along the path of the incident particle (called the track etch rate V_t) and a constant rate in all other regions (called the bulk etch rate V_b). All models of track growth are based on these two parameters which were introduced by Fleischer et al. (1975).

During etching, the track development passes through several phases. At the beginning of etching, the track is conical with a sharp tip. If etching passes the end point of the particle trajectory, the track tip becomes rounded. Therefore, these two main phases can be distinguished as the sharp conical one and the rounded one. If etching is prolonged, the track can become spherical (Durrani and Bull, 1987). The track opening also passes through different phases, which were analyzed in details by Somogyi and Szalay (1973). The track opening is circular when the incident angle is 90°. For oblique incidence, the track opening is elliptical, elliptical + circular or circular depending on the etching condition, incident energy and incident angle (for a constant V_t), or semi-elliptical or an even more complex "egg-like" geometrical figure (for a varying V_t).

In the present paper, we compared four different models of track growth given by Somogyi and Szalay (1973), Fews and Henshaw (1982), Fromm et al. (1988) and Nikezic and Yu (2003a,b). All of these four models enabled calculations of the length of the major axis of the alpha-particle track openings, which was the quantity compared in the present work. Some results of our model have already been published (Nikezic and Yu, 2002, 2003b), but without comparison with experimental data.

* Corresponding author. Tel.: +381 34 336223; fax: +381 34 335040.
E-mail address: nikezic@kg.ac.yu (D. Nikezic).

1350-4487/$ - see front matter © 2005 Elsevier Ltd. All rights reserved.
doi:10.1016/j.radmeas.2005.09.006

Many other works have made partial comparisons between models of the track growth and experiment data. For example, Dörschel et al. (2003a) compared the calculated and experimentally measured profiles of tracks from alpha particles and ^{7}Li ions in the CR-39 detector. Comparisons were made for one incident energy (5.9 MeV for alpha particles and 7.95 MeV for ^{7}Li ions) and one incident angle (40° with respect to the normal to the detector surface) for two removed layers. Good agreement between the experimental and calculated profiles was found in all examined cases. Calculated and measured profiles for protons (with energy of 1.27 MeV), alpha particles (with energy 4 MeV), ^{7}Li ions (with energy of 4.82 MeV) and ^{12}C ions (with energy of 14.8 MeV) were also compared by Dörschel et al. (2003b) and again good agreements were found for two removed layers. The calculations in both these two papers were based on the model of Fromm et al. (1988).

However, there has not been systematic comparison for a whole range of incident angles and energies of alpha particles. In the present paper, systematical comparison between models and experimental results is given for whole ranges of incident angles and energies.

2. Calculation method

Four different computer programs were separately prepared for the four track growth models mentioned above. Details of the models can be found in the corresponding references so they are not repeated here. Comparisons were made for alpha-particle tracks in the CR-39 detector. The input parameters, V_t and V_b, given below were adopted for all models. The bulk etch rate was taken as $V_b = 1.2\,\mu m/h$ (Ho et al., 2003). The variable track etch rate V_t was taken from Yu et al. (2005) as

$$V = 1 + e^{-a_1 R' + b} - e^{-a_2 R' + b}, \quad (1)$$

where R' was the residual range of alpha particles, and the constants were $a_1 = 0.06082\,\mu m^{-1}$, $a_2 = 0.8055\,\mu m^{-1}$ and $b = 1.119$. This function was obtained by measuring the depths of sub-micron tracks in a CR-39 detector generated by alpha particles with energies from 1 to 4.5 MeV, from replicas using atomic force microscopy (Yu et al., 2005). Therefore, this function can be useful for energies up to ~ 5 MeV (or $R' \approx 28.5\,\mu m$ in the CR-39 detector).

3. Experiment

The CR-39 detectors used in the present work were purchased from Page Mouldings (Pershore) Limited (Worcestershire, England). The cut detectors were systematically irradiated with alpha particles with energies ranging from 1 to 5 MeV, with steps of 1 MeV. An ^{241}Am alpha-particle source (main initial energy $E_o = 5.48$ MeV) was employed, and the stopping medium between the source and the detectors was air. The alpha-particle energy incident on a piece of detector with a distance from the source was determined with an alpha spectroscopy system (ORTEC Model 5030). The incident angle (with respect to the detector surface) was also varied from 40° up to 90°, with steps of 10°. Irradiation with angles smaller than 40° will be close to the critical angle. Fromm et al. (1988) found that there were many cases for which a great number of tracks were missing when the incident angle was smaller than 40°.

At least three pieces of CR-39 detectors were irradiated with each combination of incident energy and angle. The irradiated detectors were etched in an aqueous 6.25 N NaOH solution at a temperature of 70° for 15 h. Under these etching conditions, the bulk etch rate has been found to be about 1.2 μm/h (Ho et al., 2003). The lengths of the major axes were measured by the Image Processing and Analysis System (Leica Imaging Systems QW in standard V2.3) with a magnification of 1000. More than 20 tracks were measured and analyzed for each combination of incident energy and angle.

4. Results

Computations of the major axes have been performed for incident angles from 40° to 90° with steps of 10°, and for four different etching times, viz., 5, 10, 15 and 20 h. Since $V_b = 1.2\,\mu m/h$ was taken, the removed layers used in calculations were 6, 12, 18 and 24 μm.

The results are given in Figs. 1–6. The same symbols are used in all figures: open circles for results from the model of Fromm et al., pluses for the Fews–Henshaw model, triangles for the Somogyi–Szalay model and solid lines for the Nikezic–Yu model. The thickness of the removed layers is given close to the corresponding groups of data.

Fig. 1 shows the results for the incident angle of 90°, where the major axis of the track opening is given as a function of the incident energy, while the etching condition is used as a parameter. One can observe good agreement among different models. Agreement is particularly good for smaller incident energies. The results from the models of Fews–Henshaw and of Fromm et al. are very close at all energies, with differences between 0.5% and 1%. The Somogyi–Szalay model agrees very well with others, but deviates slightly at larger energies. The largest difference occurs at the largest considered energy of 7 MeV and amounts up to 1.5 μm, which is 7–20% larger in comparison to the Fews–Henshaw model. The Nikezic–Yu model falls between the models of Fews–Henshaw and Fromm et al. on one side and the Somogyi–Szalay model on the other side. In fact, the same pattern appears in all investigated cases.

The results for the incident angle of 80° are given in Fig. 2. There are no qualitative differences from the results shown in Fig. 1. The difference, up to 1.5 μm (8–24%), between the models of Somogyi–Szalay and Fews–Henshaw

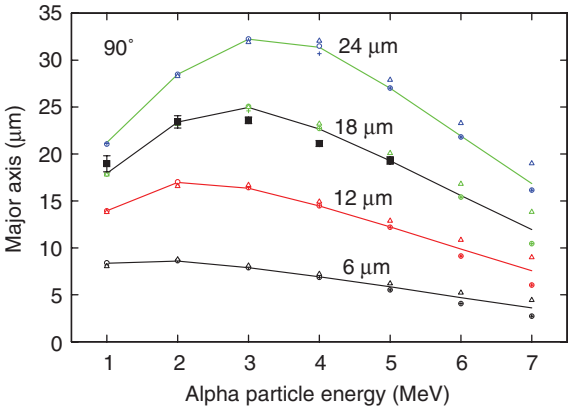

Fig. 1. Comparison of the lengths of the major axis of tracks from alpha particles with different incident energies calculated by four different track growth models for the incident angle 90° with experimental data. Open circles: results from the model of Fromm et al. (1988); Pluses: results from the model of Fews and Henshaw (1982); Triangles: results from the model of Somogyi and Szalay (1973); Solid lines: results from the model of Nikezic and Yu (2003 a, b); Solid squares: experimental data with error bars showing one standard deviations. The removed layers are 6, 12, 18 and 24 μm as shown.

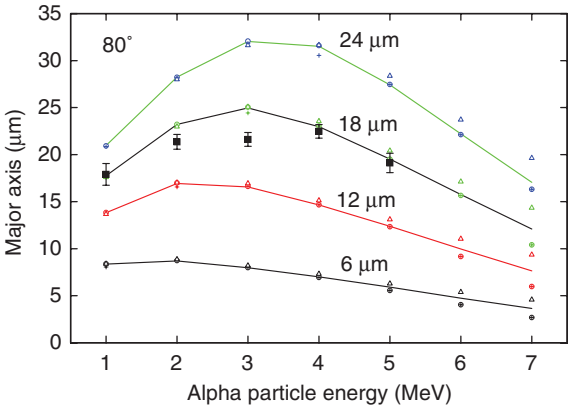

Fig. 2. Same as Fig. 1, but for the incident angle 80°.

is again largest at 7 MeV. The Nikezic–Yu model also falls between those two. The differences become smaller and all models converge for smaller energies.

For smaller incident angles (see Figs. 3–5), the discrepancies among the models increase, but not significantly. For the incident angle of 40° (Fig. 6), some data are missing because the programs do not produce results for some of the models. The poorest agreement for the incident angle of 40° (Fig. 6) occurs at the right end of the curves (for incident energies of 5, 6 and 7 MeV) where the Fews–Henshaw and Fromm et al. models gave smaller values than the Somogyi–Szalay and Nikezic–Yu models. This is consequence of different

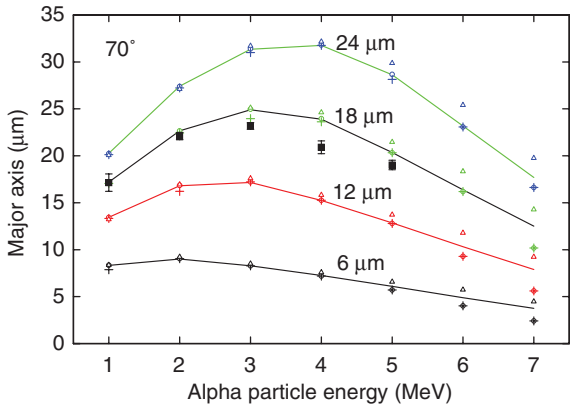

Fig. 3. Same as Fig. 1, but for the incident angle 70°.

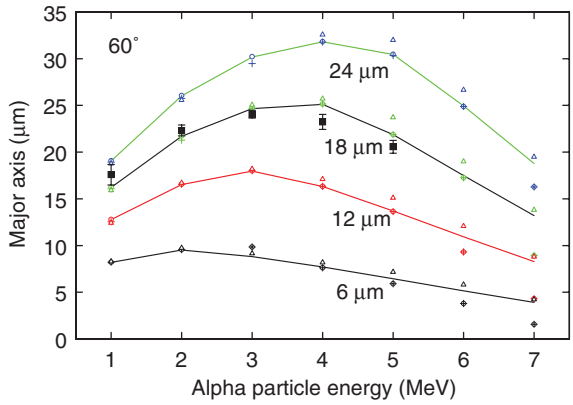

Fig. 4. Same as Fig. 1, but for the incident angle 60°.

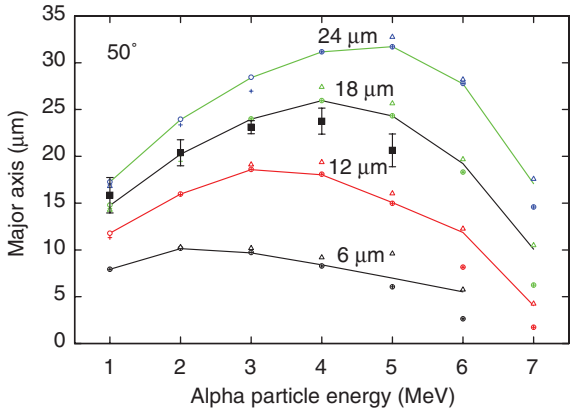

Fig. 5. Same as Fig. 1, but for the incident angle 50°.

treatments of the tracks whose developments do not start on the initial surface of the detector. In the lower energy region, agreement is also very good for the incident angle of 40°.

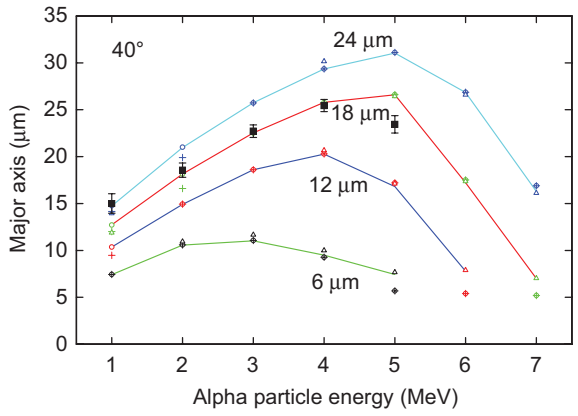

Fig. 6. Same as Fig. 1, but for the incident angle 40°.

Comparisons with experimental results are also given in Figs. 1–6. Experimental data are represented by solid squares and these correspond to a removed layer of 18 µm. There are no observed systematic discrepancies between the calculated and the experimental values. In all examined cases, the discrepancies are smaller than 20%; and in some cases these are even below 5%.

5. Conclusions

Comparison of track growth models through the prediction of the lengths of the major axis has shown small differences among the four examined models. The models from Fews–Henshaw and Fromm et al. agree within less than 1% and the results overlap for all the examined incident energies, incident angles and removed layers. The Somogyi–Szalay model gives consistently larger values for the major axis for larger incident energies while the Nikezic–Yu model consistently falls between the two extreme cases. The general conclusion is that these models give practically the same values for the major axis of the track opening for wide ranges of incident angles and removed layer, for incident alpha energies up to 5 MeV. For incident alpha energies larger than 5 MeV, discrepancies among models become apparent. These are likely due to the inherent different approaches of the different models, and will be the subject of a separate investigation in the future. Finally, the values calculated using different models of track growth agree with the experimental data to within 20%.

Acknowledgements

The present research was supported by the Serbian Ministry of Science Technology and Development through the project no. 1425, and by the Research Grants Council of Hong Kong through the project CityU 102803 (City University reference 9040882).

References

Ditlov, V., 1995. Calculated tracks in plastics and crystals. Radiat. Meas. 25, 89–94.

Dörschel, B., Hermsdorf, D., Reichelt, U., Starke, S., Wang, Y., 2003a. 3D computation of the shape of etched tracks in CR-39 for oblique particle incidence and comparison with experimental results. Radiat. Meas. 37, 563–571.

Dörschel, B., Hermsdorf, D., Reichelt, U., Starke, S., 2003b. Computation of etched track profiles in CR-39 and comparison with experimental results for light ions of different kinds and energies. Radiat. Meas. 37, 573–582.

Durrani, S.A., Bull, R.K., 1987. Solid State Nuclear Track Detection: Principles, Methods and Applications. Pergamon Press, Oxford.

Fews, A.P., Henshaw, D.L., 1982. High resolution alpha spectroscopy using CR-39 plastic track detector. Nucl. Instrum. Methods 197, 517–529.

Fleischer, R.L., Price, P.B., Walker, R.M., 1975. Nuclear Tracks in Solids. University of California Press, Berkley.

Fromm, M., Chambaudet, A., Membrey, F., 1988. Data bank for alpha particle tracks in CR39 with energies ranging from 0.5 to 5 MeV recording for various incident angles. Nucl. Tracks Radiat. Meas. 15, 115–118.

Henke, P.R., Benton, E., 1971. On geometry of tracks in dielectric nuclear track detector. Nucl. Instrum. Methods 97, 483–489.

Ho, J.P.Y., Yip, C.W.Y., Nikezic, D., Yu, K.N., 2003. Effects of stirring on the bulk etch rate of CR-39 detector. Radiat. Meas. 36, 141–143.

Nikezic, D., Kostic, D., 1997. Simulation of the track growth and determination the track parameters. Radiat. Meas. 28, 185–190.

Nikezic, D., Yu, K.N., 2002. Profiles and parameters of tracks in the LR115 detector irradiated with alpha particles. Nucl. Instrum. Methods Phys. Res. B 196, 105–112.

Nikezic, D., Yu, K.N., 2003a. Three-dimensional analytical determination of the track parameters. Over-etched tracks. Radiat. Meas. 37, 39–45.

Nikezic, D., Yu, K.N., 2003b. Calculations of track parameters and plots of track openings and wall profiles in CR-39 detector. Radiat. Meas. 37, 595–601.

Nikezic, D., Yu, K.N., 2004. Formation and growth of tracks in nuclear track materials. Mater. Sci. Eng. R 46, 51–123.

Paretzke, G.H., Benton, E., Henke, P.R., 1973. On the particle track evolution in dielectric track detectors and charge identification through track radius measurements. Nucl. Instrum. Methods 108, 73–80.

Somogyi, G., 1980. Development of etched nuclear tracks. Nucl. Instrum. Methods 173, 21–42.

Somogyi, G., Szalay, A.S., 1973. Track diameter kinetics in dielectric track detector. Nucl. Instrum. Methods 109, 211–232.

Yu, K.N., Ng, F.M.F., Nikezic, D., 2005. Measuring depths of submicron tracks in a CR-39 detector from replicas using Atomic Force Microscopy. Radiat. Meas. (Available online on 5 July 2005 on www.sciencedirect.com), in press.